CARACTERÍSTICAS MICROESTRUTURAIS, MODOS DE FALHA E PROPRIEDADES MECÂNICAS DE AÇOS TWIP SOLDADOS POR SOLDAGEM A PONTO POR RESISTÊNCIA

*

Tiago Cristofer Aguzzoli Colombo[1]
Guilherme José dos Santos[2]
Jorge Otubo[3]
Alfredo Rocha de Faria[4]

Resumo
Chapas de aço TWIP980 foram soldadas por soldagem a ponto por resistência com diferentes parâmetros de processo. A microestrutura pós-soldagem foi caracterizada e as propriedades mecânicas das juntas soldadas foram avaliadas. Para cada condição de processo, os modos de falha foram identificados e correlacionados com as propriedades mecânicas. Não foram identificadas regiões de segregação de manganês, indicando que o material pós-soldado mantém sua microestrutura austenítica, o que foi confirmado por difractogramas de raios-x e micrografias ópticas.Mapas de microindentação mostraram uma distribuição heterogênea de propriedades mecânicas ao longo da junta soldada. Além disto, a região mais macia localiza-se na zona de fusão da solda, favorecendo modos de falha frágeis, o que foi identificado através de ensaios mecânicos de tração-cisalhamento. No entanto, ajustes de parâmetros de processo mostraram-se eficazes para promover outros modos de falhas, inclusive falha dúctil, o que foi confirmado através de micrografias eletrônicas. Os resultados também mostraram que a resistência mecânica e a capacidade de absorção de energia das juntas estão diretamente relacionados com os parâmetros de processo e modos de falha.
Palavras-chave:Aço TWIP; AHSS; Resistance Spot Welding; TWIP steel; Failure Modes

MICROSTRUCTURAL FEATURES, FAILURE MODES AND MECHANICAL PROPERTIES OF RESISTANCE SPOT WELDED TWIP STEELS

Abstract
TWIP980 steel sheets were welded by resistance spot welding with different welding parameters. The as-welded microstructure was characterized and the mechanical properties of the weld spots were assessed. For each welding condition, the failure modes were identified and correlated with the mechanical properties. No considerable Mn segregation was identified, indicating that the material remains essentially austenitic in the as-welded condition, which was confirmed by XRD patterns and optical micrographs. The fusion zone hardness is lower than that of heat affected zone and base metal, as evidenced by microindentation maps, which facilitates interfacial failure mode during tensile-shear tests. However, adjustments in the process parameters were shown to be effective in promoting more favorable

failure modes, which was confirmed by scanning electron micrographs. The results also showed that the tensile-shear strength and energy absorption capability are directly correlated to the failure modes and the welding process parameters.
Keywords: TWIP steel; AHSS; Resistance Spot Welding; Failure Modes

[1] *Engenheiro de Materiais, Mestre em Engenharia Metalúrgica, Doutorando noDepartamento de Engenharia Aeronáutica e Mecânica, Instituto Tecnológico de Aeronáutica, São José dos Campos, São Paulo,Brasil.*
[2] *Engenheiro de Materiais, Mestrando noDepartamento de Engenharia Aeronáutica e Mecânica, Instituto Tecnológico de Aeronáutica, São José dos Campos, São Paulo, Brasil.*
[3] *Graduação em Física, Doutor em Engenharia Mecânica, Professor Associado doDepartamento de Engenharia Aeronáutica e Mecânica, Instituto Tecnológico de Aeronáutica, São José dos Campos, São Paulo, Brasil.*
[4] *Engenheiro Mecânico, Doutor em Engenharia Aeroespacial, Professor Associado doDepartamento de Engenharia Aeronáutica e Mecânica, Instituto Tecnológico de Aeronáutica, São José dos Campos, São Paulo, Brasil.*

1 INTRODUCTION

Advanced High-Strength Steels (AHSS) with twinning-induced plasticity (TWIP) effect have gained increasing importance in the transportation industry due to their combination of very high yield and ultimate tensile strength with elevated ductility, yet keeping cold formability [1, 2]. Such properties are desirable to increase strength and decrease weight of critical components by using thinner and formable steel sheets. Due to their technological importance, many studies have been conducted to investigate the microstructure evolution and formability of these steels [1-4].

Following the sheet forming processes, individual components in transportation industry are usually assembled by means of joining processes. Among the joining processes applied in automotive body-in-white manufacturing, resistance spot welding (RSW) is considered the dominant one, mainly due to its low-cost, ease of automation and robustness [5, 6].The quality of the weld spots has significant influence on the structural integrity of assembled components and, in a larger perspective, on the performance of the vehicle. An adequate definition of RSW parameters has, therefore, great importance, since the quality of the weld spots has a direct impact on the quality of the weldment.

Despite the importance of the welding processes on the quality and safety of the assembled components, little has been published on the effects of RSW parameters on the quality of TWIP weld spots.Pouranvari and Marashi [7,8] state that one of the main concerns regarding the use of AHSS in RSW process is the tendency to fail in a brittle manner, exhibiting the interfacial failure mode, in which the crack propagates through the fusion zone of the weldment, especially when loaded in tensile-shear loading condition. Interfacial failure mode is not desirable for automotive applications, as it is usually associated with low plastic deformation and low load bearing capacity [7,8]. As recently stated by Rao et al. [9], the change between the brittle interfacial failure mode to ductile pullout failure (PF) mode, in which there is an increase in tensile shear strength, plastic deformation and load bearing capacity, mainly depends upon the size of the weld nugget. Therefore, changes in welding parameters in order to promote an increase in weld nugget size could result in pullout failure mode.On the other hand, Radakovic and Tumuluru [10] demonstrated that there was no significant difference between the peak load of the weld spots that failed under IF or PF mode involving Dual-Phase (DP) and Transformation-Induced Plasticity (TRIP) steels.

The aforementioned few publications on spot-welded AHSS steels provide meaningful contributions to the state of the art regarding the microstructure evolution and mechanical properties during RSW process. Nonetheless, they do not yet fully satisfy the gap on the subject when involving TWIP steels, as investigations covering a larger range of welding parameters and their impact on failure modes and so on mechanical properties were not performed.

In the light of the above, the aim of this paper is to understand the relationship between process-microstructure-mechanical behavior of TWIP steel weld spots, emphasizing the correlation between welding parameters, microstructure and mechanical properties evolution and failure modes.

2 MATERIALS AND METHODS

2.1 Materials

Experimental investigations were conducted with uncoated cold rolled 0.8 mm thick Fe–Mn–C–Si–Al austenitic TWIP980 steel sheets with the chemical composition shown in Table 1. The microstructure at room temperature is fully austenitic, with an average grain size of 2.5 μm.

Table 1. Chemical composition of the investigated steel (wt.%)

C	Mn	Al	Ti	Cr	Mo	Si	Ni	Fe
0.75	16.4	1.91	0.10	0.72	0.26	0.05	0.03	Bal.

2.1 Welding procedures

Weldings were conducted using a Düring CB 150 kvA spot welding machine, a Harms &WendeRatia 73 welding panel and a copper electrode with a face diameter of 6.0 mm with constant water cooling flow rate of 6 $l.min^{-1}$. The welding current was varied from 5 to 8 kA with a step of 1kA. Electrode force varied from 2 kN to 4 kN with a step of 2 kN. Welding time varied from 8 cycles to 16 cycles, with a step of 4 cycles. Squeeze time and holding time were set as 32 and 12 cycles.

2.2Characterization methods

Quasi-static tensile-shear tests were performed using an electromechanical Instron Universal Testing Machine at a cross head speed of 10 $mm.min^{-1}$.The mechanical strength of the weld spots was investigated and compared to each welding current interval by analyzing the load vs. displacement curves obtained from tensile-shear tests up to maximum tensile-shear load. Weld spot diameter and the indentation depth caused by electrode penetration during welding were measured using a Cyber CT-100 non-contact profilometer. Conventional metallographical procedures and optical microscopy observations were conducted to reveal the fusion zone (FZ) size of the weld spots and the metallurgical microstructuresalong the Base Metal (BM), Heat Affected Zone (HAZ) and FZ. Vickers hardnessmaps were carried out on the polished samples under an indentation load of 1 N and grid spacing 62.5 μm,using a Emcotest hardness tester. The fractured surfaces of the tensile tested samples were investigated by scanning electron microscopy (SEM) using a TESCAN VEGA 3 XMU microscope in the secondary electron imaging mode.

3 RESULTS AND DISCUSSION

3.1Microstructural features of the weld spots

A typical hardness map of a TWIP steel weld spot is shown in **Erro! Fonte de referência não encontrada.**a (half of the cross section of a weld spot). It is possible to observe that the hardness increases from the Base Material (BM) towards the HAZ, where it achieves its highest values, and then decreases from the HAZ towards

the FZ. A possible explanation for a lower hardness at the FZ may be due to the as-cast grain morphology of the FZ, which can be seen in **Erro! Fonte de referência não encontrada.**b. The FZ grain morphology consists of columnar dendritic grain structure with grains oriented preferentially in the thermal gradient direction, normal to the solid/liquid interface (from the weld centerline towards the sheet-electrode surfaces and HAZ). On the other hand, the HAZ (**Erro! Fonte de referência não encontrada.**c) preserves the equiaxed grain structure of the base material (**Erro! Fonte de referência não encontrada.**d), although it is possible to observe a grain coarsening due to the high temperatures the HAZ experienced during the welding cycle. The average grain size at the HAZ, obtained from a linear intercept method, is 8.5 µm, more than 3x higher than the grain size of the BM, which is around 2.5 µm.

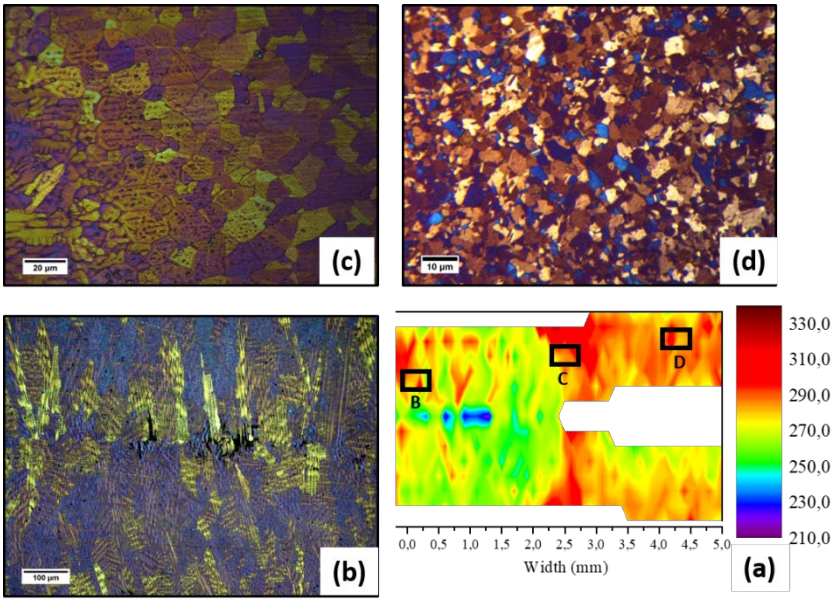

Figure 1. Representative microstructural features of a weld spot: (a) hardness map, (b) grain morphology of the FZ, (c) grain morphology of the HAZ and (d) grain morphology of the BM.

Although the HAZ has a coarser grain structure when compared to the BM, it is also harder than the BM. During the welding period, the expanding FZ dislocates the surrounding material, causing displacements of the sheet metal. On cooling period, the weldment is submitted to cooling rates as high as those reached during the quenching process, which causes the FZ to pull the surrounding area. However, the cooling of the HAZ leads to an increase in its Young's modulus which makes it difficult to be brought back by the tensile stress arisen during cooling[11]. As TWIP steel exhibit high work hardening coefficient, the thermomechanical loads that arise at the HAZ during the welding cycle may be enough to work harden the material, causing the increase in HAZ observed in **Erro! Fonte de referência não encontrada.**a.

It is possible to observe a region of small equiaxed grains adjacent to the FZ. According to Sahaet al.[6], the small equiaxed grain region is the result of incomplete fusion of the BM at this point, promoting the occurrence of a partially molten zone (PMZ), which is a favorable failure site. Differently than the observed by Saha et al. [6], it was not observed liquation cracks at the HAZ, which may be due to the absence of Zn coating in the TWIP steel investigated in the present study.

EDS images of the elemental distribution of Fe, Mn, Al, O, Si, Ti, C and N taken from the weld centerline are shown in **Erro! Fonte de referência não encontrada.**.A

concern was raised by Saha et al. [6] regarding the tendency of C and Mn to segregate at the weld spot center line, which is the last region to solidify. An indication of Mn segregation was also reported by Mujica et al. [12] for laser welded TWIP steels. The stabilization of austenite at room temperature of TWIP steels is due to its high Mn content. Its segregation may lead to undesirable phase transformations during the welding cycle, especially martensitic transformation due to its high C content. Martensitic transformation may be undesirable in TWIP steels for three main reasons: (i) it is a source of tensile residual stresses, as volumetric changes are associated with it, (ii) the material may lose its twinning capacity, which is responsible for the combination of high strength and ductility that characterizes the material and (iii) martensite transformationimpairs toughness and also may facilitate the occurrence of delayed fracture, which has also been reported for TWIP steels [13–15].

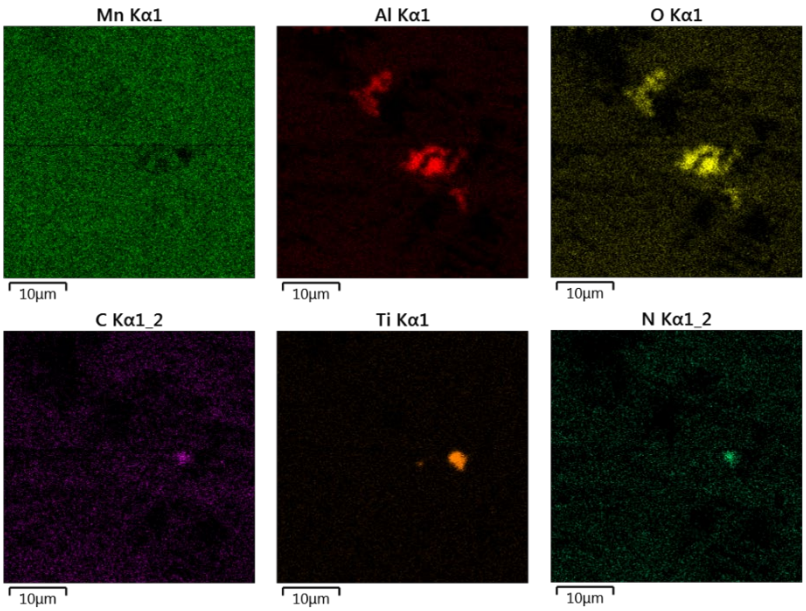

Figure 2.EDS maps for elements Fe, Mn, Al, O, Si, Ti, C and N.

As can be seen in **Erro! Fonte de referência não encontrada.**, both C and Mn did not exhibit noticeable segregation, which differs from the results found by Saha et al. [6]. A possible explanation is the higher thickness of the TWIP sheets in the study of Saha et al. [6]. It is expected that the cooling rate is higher for thinner sheets, which in turn hinders diffusion of alloying elements. On the other hand, it is possible to observe high concentrations of Al and O in specific regions, indicating the presence of aluminum oxide. Al segregation may be a concern as Al has two main roles in the chemical composition of TWIP steels: suppress cementite precipitation by reducing the activity and diffusivity of C in austenite and suppress strain-induced martensitic transformation by increasing the SFE[2,16]. Therefore, Al segregation may decrease the austenite stability in the adjacent regions, facilitating undesirable phase transformations if the material is subjected by further cyclic loading.

Figure 3 shows XRD patterns for the base metal and for the as-welded material. The results from XRD analysis indicate that the welding process did not promote the formation of different metallurgical phases other than austenite. It is in agreement with the absence of Mn segregation observed by EDS analysis (Fig 2).However, it is possible to observe a shift and broadening of the characteristic austenite peaks, which may be an indicative of residual stresses arising during the welding cycles.

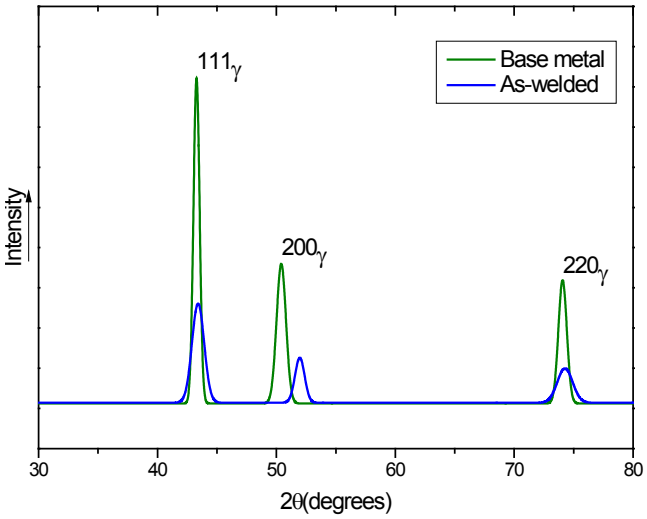

Figure 3.XRD patterns for the base metal and weld spot.

3.2Failure Modes

The quality of the weld spots has significant influence on the structural integrity and reliability of the vehicle and, in a large scale, on the passenger safety. One of the main indicatives of the weld spot quality is its failure mode. Therefore, an understanding on how RSW parameters may affect mechanical behavior and failure modes of AHSS is of technological interest, as unfavorable failure modes may impair the sophisticated mechanical properties of AHSS, thus requiring a large number of weld spots to ensure structural integrity. On the other hand, any optimization in the RSW process towards an improvement on the quality of weld spots may also represent productivity gains on floor shop [7, 8, 11].

The SEM micrographs of fracture surfaces for different welded samples are shown in **Erro! Fonte de referência não encontrada.**. For welding currents up to 6 kA, the samples exhibited the typical brittle IF mode, with crack propagation through the weld nugget (**Erro! Fonte de referência não encontrada.**a). It is possible to observe the flatness of the surface, indicating little plastic deformation, combined with the presence of torn bands visible by SEM, which are associated to a quasi-cleavage fracture, typical of a brittle fracture mechanism [17]. When higher heat inputs are applied (welding current of 8 kA), it is possible to identify a change in the failure mode. The failure occurs predominantly by the withdrawal of the weld spot from one sheet, preferentially through the HAZ around the weld nugget, accompanied by a considerable amount of plastic deformation before complete failure (**Erro! Fonte de referência não encontrada.**b). The weld nugget itself remained intact under mechanical loading. The fracture surface exhibits equiaxed dimples at the HAZ, which is associated with a ductile failure mechanism [17]. It is possible to identify small dimples combined with larger and deeper ones. Pouranvari et al.[7]stated that both nugget size and hardness ratio of FZ to pullout failure location most influence the failure mode of RSWs. The larger is the nugget size, the lower the shear stress at the sheet-sheet interface, facilitating the occurrence of ductile PF mode.

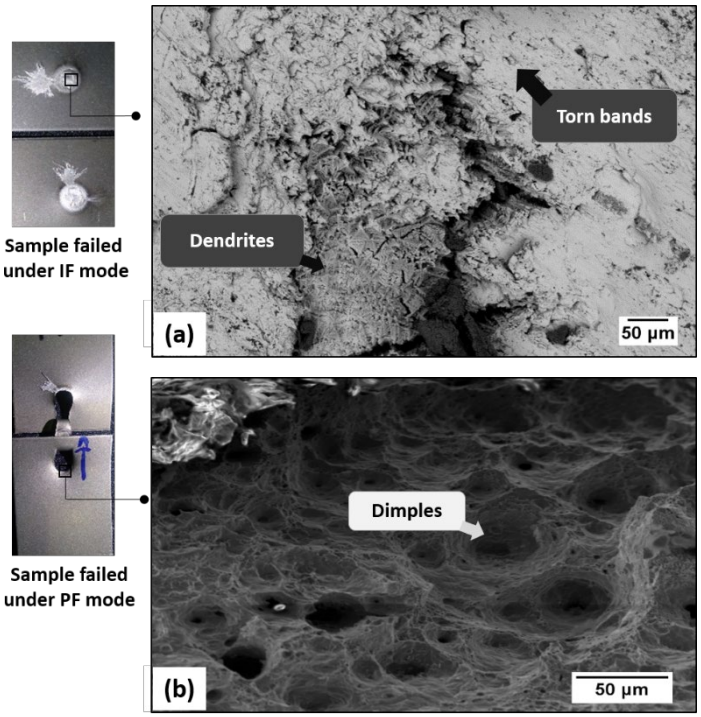

Figure4. Scanning electron micrographs evidencing: (a) a brittle fracture surface of a sample that failed under IF mode and (b) a ductile fracture surface of a sample that failed under PF mode.

Hardness, in turn, has a strong influence on the failure mode as the necking during tensile shear loading tends to occur preferentially where hardness is lower. The higher the hardness of the FZ relative to the hardness of HAZ or BM, the higher is the chance of PF mode in detriment of IF mode, as it provides a preferential location for necking during the tensile-shear loading [7]. As shown in **Erro! Fonte de referência não encontrada.**a, the FZ hardness of the TWIP steel welded samples is lower than the hardness of BM or HAZ. Therefore, it is reasonable to presume that the increase in nugget size at 8 kA is the driving force to promote the change in failure mode. Although previous studies in literature stated that TWIP steels tend to fail only in IF (brittle) mode, the present results show that it is possible to achieve a favorable failure mode if adequate nugget size is achieved.

When intermediate heat inputs are applied (7 kA), the weld spots subjected to tensile-shear loading exhibited the partial interfacial failure (PIF) mode, in which the crack initially propagates through the FZ at approximately 45 degrees of the surface plane and then redirects through the thickness direction [9, 18]. **Erro! Fonte de referência não encontrada.**ashows the macrograph of a weld spot which failed under PIF mode. The SEM micrograph of the flat part of the fracture surface, marked as Box A, is enlarged in **Erro! Fonte de referência não encontrada.**b, where it is possible to observe depressions caused by the propagating crack and large shrinkage voids. An insufficient molten metal volume, which may be caused by low heat input and/or molten expulsion, may cause the formation of shrinkage voids and cracks. When the Box B is enlarged (**Erro! Fonte de referência não encontrada.**c), dendrites are visible on the surface of these large voids. These dendrites exhibit the characteristics of free solidification structure, as they consume the last solidifying liquid during cooling. Free solidification structures associated to insufficient molten metal volume may act as facilitating crack nucleation and propagation during mechanical loading, thus providing low mechanical strength for the weld nugget, even if adequate weld nugget size is achieved.

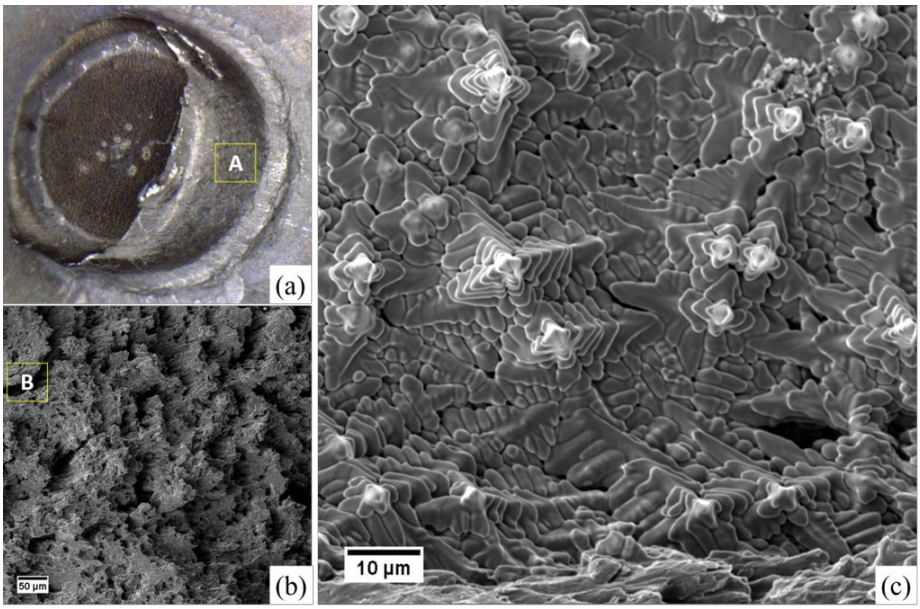

Figure5. Observations of the fracture surface, I = 7 kA: (a) macrograph evidencing PIF mode, (b) SEM micrograph of the region marked as box A and (c) SEM micrograph of box B.

3.3Tensile-shear strength

Figure 7 shows the tensile-shear strength of the weld spots as a function of welding current and electrode force. It is possible to observe that the tensile-shear strength continuously increases with increasing the welding current. According to Pouranvari and Marashi [7], spot welding of AHSS is governed by the same overall Joule effect principle as mild steels, with welding nugget size increasing with the welding current applied. It is possible to observe that the highest mechanical strength values are found for the weld spots that failed under PF mode (8kA).

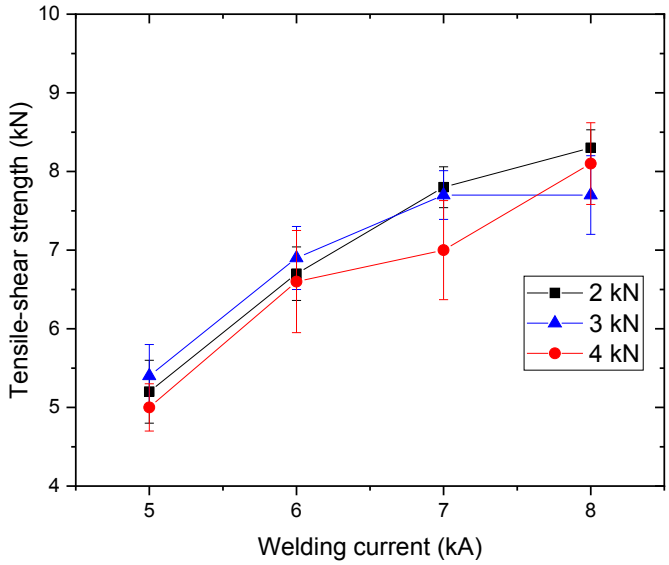

Figure7. Mechanical properties of the weld spots as a function of welding current and electrode force. Welding time = 8 cycles.

An increase in the electrode compression force from 2 kN to 3 kN seems to have negligible impact on tensile-shear strength, at least for welding currents up to 7 kA. On the other hand, when an electrode compression force of 4 kN is applied, the tensile-shear strength tends to decrease. It is also possible to observe a higher dispersion in the mean values of mechanical strength when higher electrode forces are applied. It may indicate an instability of the mechanical reliability when higher electrode forces are applied, which may be possibility due to the more intense macroscopic (increase in electrode indentation depth) and microstructural (work hardening) changes that an increase in electrode force promotes[11].
An increase in welding time, on the other hand, promotes an increase in tensile-shear strength for all the welding current values, as shown in Fig. 8. It may be due to the increase in heat input and thus in weld spot size by increasing welding time, according to the Joule effect principle [7, 11]. Although longer welding times may also promote more pronounced grain coarsening in the material, this does not appear to affect the mechanical properties of the weld spot, at least in a quasi-static loading point-of-view.

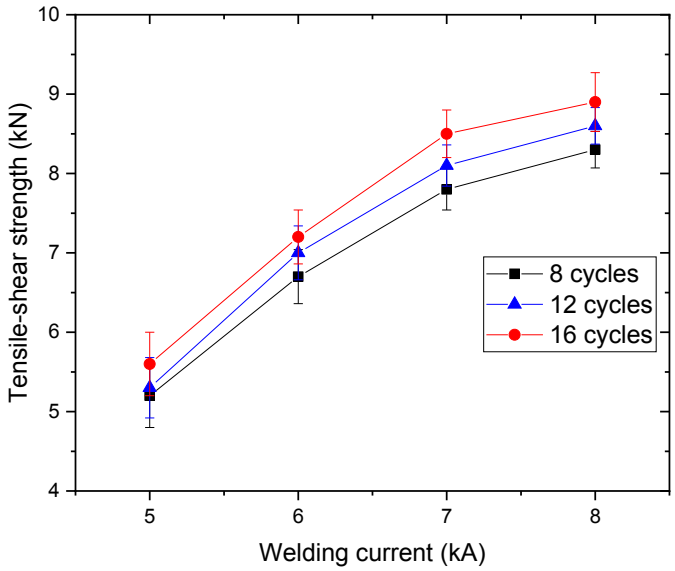

Figure8. Mechanical properties of the weld spots as a function of welding current and welding time. Electrode force = 2 kN.

4 CONCLUSIONS

The following conclusions can be drawn from the results obtained by the experimental investigations conducted in this work:

- The microstructure of the weld spots consisted of a well-defined dendritic FZ, a coarse grained HAZ and a narrow PMZ. No considerable Mninterdendritic segregation was observed and XRD patterns and optical micrographs showed that the resulting microstructure of the weld spots remains essentially austenitic.
- When welding currents up to 6 kA were applied, the weld spots failed under interfacial (brittle) failure, confirmed by the cleavage fracture surface evidenced by SEM micrographs. On the other hand,for welding currents of 8 kA, the respective weld spots underwent pullout (ductile) failure, confirmed by

the dimpled fracture surface observed by SEM. The transition from brittle to ductile failure occurs when 7 kA were applied.

- The results demonstrate that it is possible to adjust process conditions that promote increase in nugget size in order to facilitate the occurrence of preferentially PF mode for the investigated TWIP steel alloy.
- An increase in welding current is always accompanied by an increase in tensile-shear strength, which was also observed when higher welding times were applied. On the other hand, an increase in electrode compression force tends to have an opposite effect on mechanical properties.

Acknowledgements

The authors would like to acknowledge the financial support provided by the Brazilian Federal Agency CAPES.

REFERENCES

1 Beladi H, Timokhina IB, Estrin Y, et al. Orientation dependence of twinning and strain hardening behaviour of a high manganese twinning induced plasticity steel with polycrystalline structure. Acta Mater. 2011;59:7787–7799.
2 Kim J, Lee SJ, De Cooman BC. Effect of Al on the stacking fault energy of Fe-18Mn-0.6C twinning-induced plasticity. Scr. Mater. 2011;65:363–366.
3 Chin KG, Kang CY, Shin SY, et al. Effects of Al addition on deformation and fracture mechanisms in two high manganese TWIP steels. Mater. Sci. Eng. A. 2011;528:2922–2928.
4 De Cooman BC, Kim J, Lee S. Heterogeneous deformation in twinning-induced plasticity steel. Scr. Mater. 2012;66:986–991.
5 Chabok A, van der Aa E, De Hosson JTM, et al. Mechanical behavior and failure mechanism of resistance spot welded DP1000 dual phase steel. Mater. Des. 2017;124:171–182.
6 Saha DC, Cho Y, Park Y-D. Metallographic and fracture characteristics of resistance spot welded TWIP steels. Sci. Technol. Weld. Join. 2013;18:711–720.
7 Pouranvari M, Marashi SPH. Failure mode transition in AHSS resistance spot welds. Part I. Controlling factors. Mater. Sci. Eng. A. 2011;528:8337–8343.
8 Pouranvari M, Marashi SPH, Safanama DS. Failure mode transition in AHSS resistance spot welds. Part II: Experimental investigation and model validation. Mater. Sci. Eng. A 2011;528:8344–8352.
9 Rao SS, Chhibber R, Arora KS, et al. Resistance spot welding of galvannealed high strength interstitial free steel. J. Mater. Process. Technol.. 2017;246:252–261.
10 Radakovic DJ, Tumuluru M. Predicting Resistance Spot Weld Failure Modes in Shear Tension Tests of Advanced High-Strength Automotive Steels. Weld. J. 2008;87:96S–105S.
11 Zhang H, Senkara J. Resistance Welding: Fundamentals and Applications. 2nd ed. CRC Press; 2011.
12 Mujica L, Weber S, Thomy C, et al. Microstructure and mechanical properties of laser welded austenitic high manganese steels. Sci. Technol. Weld. Join. 2009;14:517–522.
13 Kim JG, Hong S, Anjabin N, et al. Dynamic strain aging of twinning-induced plasticity (TWIP) steel in tensile testing and deep drawing. Mater. Sci. Eng. A 2015;633:136–143..

14 Pranke K, Wendler M, Weidner A, et al. Formability of strong metastable Fe-15Cr-3Mn-3Ni-0.2C-0.1N austenitic TRIP/(TWIP) steel - A comparison of different base materials. J. Alloys Compd.2015;648:783–793..
15 Hwang JK, Yi IC, Son IH, et al. Microstructural evolution and deformation behavior of twinning-induced plasticity (TWIP) steel during wire drawing. Mater. Sci. Eng. A. 2015;644:41–52.
16 Jin JE, Lee YK. Effects of Al on microstructure and tensile properties of C-bearing high Mn TWIP steel. Acta Mater. 2012;60:1680–1688.
17 Yuan X, Li C, Chen J, et al. Resistance spot welding of dissimilar DP600 and DC54D steels. J. Mater. Process. Technol. 2017;239:31–41.
18 Pouranvari M, Marashi SPH. Critical review of automotive steels spot welding: process, structure and properties. Sci. Technol. Weld. Join. 2013;18:361–403